narra j

**Original Article**

# Dual anti-inflammatory and antimicrobial effects of stingless bee propolis on second-degree burns

**Christian O. Manginstar[1,2,3], Trina E. Tallei[4,5*], Christina L. Salaki[1], Nurdjannah J. Niode[6,7] and Hendra K. Jaya[8]**

[1]Postgraduate Program, Department of Entomology, Universitas Sam Ratulangi, Manado, Indonesia; [2]Division of Surgical Oncology, Department of Surgery, Faculty of Medicine, Universitas Sam Ratulangi, Indonesia; [3]Division of Surgical Oncology, Department of Surgery, Prof. Dr. R.D. Kandou Hospital, Manado, Indonesia; [4]Department of Biology, Faculty of Mathematics and Natural Science, Universitas Sam Ratulangi, Manado, Indonesia; [5]Department of Biology, Faculty of Medicine, Universitas Sam Ratulangi, Manado, Indonesia; [6]Department of Dermatology and Venereology, Faculty of Medicine, Universitas Sam Ratulangi, Manado, Indonesia; [7]Department of Dermatology and Venereology, Prof. Dr. R.D. Kandou Hospital, Manado, Indonesia; [8]Institut Citra Internasional, Pangkalpinang, Indonesia

*Corresponding author: trina_tallei@unsrat.ac.id

## Abstract

Propolis, a natural resinous product from stingless bees, is widely recognized for its anti-inflammatory and antimicrobial properties. However, its combined effects in addressing both inflammation and infection in second-degree burns have remained insufficiently explored. The aim of this study was to investigate the dual role of propolis in modulating inflammation and preventing bacterial infections caused by methicillin-resistant *Staphylococcus aureus* (MRSA) and *Pseudomonas aeruginosa* in a second-degree burn model. Propolis was collected from stingless bees in Gowa, South Sulawesi, Indonesia, and extracted using methanol. Second-degree burns were induced in male *Rattus norvegicus*, which were then divided into three groups: one treated with propolis, another silver sulfadiazine (positive control), and third with NaCl (negative control). After seven days of treatment, the expression of tumor necrosis factor-alpha (TNF-α) and vascular endothelial growth factor (VEGF) proteins in wound samples was analyzed using immunohistochemistry. The antimicrobial activity of the propolis extract was assessed using the disc diffusion assay, followed by minimum inhibitory concentration (MIC) testing. Network pharmacology analysis was also conducted to assess the anti-inflammatory activity of propolis. Results showed that propolis significantly reduced TNF-α expression and increased VEGF expression, which might enhance VEGF-mediated angiogenesis, leading to improved wound healing compared to controls. The antimicrobial tests demonstrated strong activity against MRSA and *P. aeruginosa*, with inhibition zones correlating with higher extract concentrations. The MIC value of the propolis extract was 198.66 µg/µL against MRSA and 212.06 µg/µL against *P. aeruginosa*. Network pharmacology analysis revealed key proteins, including Jun proto-oncogene (JUN), estrogen receptor 1 (ESR1), signal transducer and activator of transcription 3 (STAT3), and proto-oncogene tyrosine-protein kinase Src (SRC), involved in the regulation of TNF-α and VEGF, further supporting the synergistic effects of propolis. This study demonstrates that stingless bee propolis effectively promotes tissue regeneration and prevents infection in second-degree burns, highlighting its potential as an alternative to conventional treatments for wound care.

**Keywords**: Wound healing, propolis, TNF-α modulation, VEGF-mediated angiogenesis, network pharmacology



https://narraj.org/

**Received: February 27, 2025 - Accepted: April 11, 2025 - Published online: April 15, 2025**

## Introduction

Burn injuries, especially second-degree burns, present significant health challenges due to their complexity and the potential for severe complications [1]. Second-degree burns penetrate through the epidermis and into the dermis, causing painful blistering and exposing the wound to a higher risk of infection [2]. The inflammatory response to these injuries is intense and can lead to prolonged healing and tissue damage [2-4]. This response typically involves the release of a variety of inflammatory mediators, including cytokines such as interleukin-1 (IL-1), interleukin-6 (IL-6), and tumor necrosis factor-α (TNF-α), which drive the inflammatory process [5]. Additionally, growth factors like vascular endothelial growth factor (VEGF) and transforming growth factor-β (TGF-β) play critical roles in tissue repair and regeneration by promoting angiogenesis and fibroblast proliferation [3,6].

In burn wounds, the loss of the skin barrier leads to rapid colonization by microorganisms, further complicating the healing process [7,8]. Gram-positive bacteria such as *Staphylococcus* spp., methicillin-resistant *Staphylococcus aureus* (MRSA), and Gram-negative bacteria like *Pseudomonas aeruginosa* are common culprits in burn infections [9,10]. These pathogens thrive due to the compromised skin integrity, necessitating effective antimicrobial treatments to prevent and manage infections.

Propolis, a resinous substance produced by bees, is noted for its medicinal properties, including anti-inflammatory, antimicrobial, and wound-healing effects [11,12]. Moreover, propolis aids in wound closure, collagen synthesis, cellular proliferation, and angiogenesis, all of which contribute to tissue remodeling [13]. Stingless bees produce a distinctive type of propolis that is rich in bioactive compounds such as flavonoids, phenolics, and terpenoids [14], which exhibit significant biological activities beneficial for burn wound management [15]. Flavonoids such as pinocembrin, galangin, and pinobanksin modulate inflammatory responses and enhance microbial resistance, while phenolic compounds reduce pro-inflammatory cytokines and promote cellular healing processes [16].

Recent studies suggest that propolis mitigates inflammation and supports wound healing through various mechanisms, including the reduction of oxidative stress, modulation of immune responses, and inhibition of microbial growth [17-19]. For example, pinocembrin has been shown to promote keratinocyte proliferation and survival, partly through the activation of the mitogen-activated protein kinase (MAPK) and phosphoinositide 3-kinase (PI3K) pathways, making it a promising natural flavonoid for development as a wound-healing agent [20].

The antimicrobial properties of propolis are also attributed to its flavonoid content, which disrupts bacterial membrane integrity and reduces bacterial resistance to antibiotics [21,22]. Despite promising evidence, the potential of stingless bee propolis in treating second-degree burns remains underexplored. The aim of this study was to investigate the synergistic anti-inflammatory and antimicrobial effects of stingless bee propolis through in vitro, in vivo, and in silico approaches by evaluating its antimicrobial activity, wound-healing effects, and the molecular mechanisms underlying its bioactive compounds.

## Methods

### Source of propolis and extraction

Propolis samples were obtained from stingless bees at a meliponiculture site in Pattallassang, Gowa, South Sulawesi, Indonesia (5.2142°S, 119.5592°E). The bee species was identified using cytochrome oxidase I (COI) barcoding, revealing a 91.76% genetic similarity to *Tetragonula clypearis*, thereby confirming its classification as *Tetragonula* sp.

A total of 200 g of propolis was dissolved in 250 mL of 100% methanol (Merck Millipore, Darmstadt, Germany) and allowed to soak at room temperature. The mixture was shaken every 2–3 hours to enhance extraction. After 48 hours, the solution was filtered using Whatman No. 1 filter paper to separate the insoluble residue, yielding a clear filtrate. The filtrate was then concentrated using a Büchi Rotavapor R-300 rotary evaporator (Büchi Labortechnik AG, Flawil, Switzerland) at 40°C under reduced pressure (100–250 mbar) to remove the methanol solvent efficiently. The evaporation was performed at a rotation speed of 100–150 rpm, with the cooling

system set between -5 and 10°C to facilitate solvent condensation. The process continued for 2–3 hours until a thick, concentrated propolis extract was obtained. The extract was then collected and stored in an amber glass container at 4°C until further analysis.

## Anti-inflammatory effects of propolis

### *Study design*

This study aimed to evaluate the anti-inflammatory and wound-healing effects of propolis extract on second-degree burn wounds in rats. The experimental design included three groups: burns treated with propolis extract as the treatment group, burns treated with 1% silver sulfadiazine as the positive control, and burns treated with 0.9% NaCl as the negative control. Following a 7-day observation period, skin samples were collected for immunohistochemical analysis of TNF-α and VEGF expression. Burn wound healing was assessed by measuring wound area, evaluating granulation tissue formation, and determining the extent of epithelialization.

### *Animals*

The animal models consisted of healthy male white rats (*Rattus norvegicus*), aged 3–4 months and weighing between 180 and 300 grams. All rats were confirmed to be in good health, exhibiting normal behavior, activity, and physical appearance. They showed no visible anatomical abnormalities and had healthy fur, free from signs of dullness, shedding, or baldness. During the acclimatization period, the average body weight of rats varied across groups, with the propolis-treated group averaging 234.4 g, the 1% silver sulfadiazine group averaging 226.7 g, and the 0.9% NaCl group averaging 228.9 g. A total of 27 rats were used in the study, with nine rats per group, as determined using the Federer formula [23].

### *Housing and husbandry*

The rats were housed in identical cages measuring 45×30×20 cm within a controlled environment to maintain consistent temperature and humidity levels, which are essential for burn wound healing. To ensure uniform nutrition, all rats were fed B-195 livestock feed at 5 g/100 g body weight (BW) per day, with water *ad libitum*. They were housed individually in clean cages with rice husk bedding, maintained at a stable temperature of 25°C. Only healthy rats without visible deformities or signs of illness were selected to maintain immune status consistency across the groups. Additionally, the rats' activity levels were monitored, and their movement was restricted as necessary to ensure uniform physical activity among all subjects.

### *Second-degree burn creation procedure*

Prior to induction, the fur on the dorsal area of the rat was shaved, and the skin surface was disinfected with 70% ethanol. The second-degree burn was induced using a modified version of a previously established protocol [24]. Briefly, a 2-cm diameter stainless-steel plate was preheated for five minutes and then applied to the skin for five seconds to produce standardized second-degree burns [25].

### *Study groups and treatments*

A total of 27 male rats were divided into three groups: Group I received a topical application of propolis extract, Group II was treated with 1% silver sulfadiazine, and Group III was administered 0.9% NaCl. Following treatment, wounds were covered with sterile gauze and secured with adhesive tape. Treatments were applied twice daily over a 7-day period, with continuous monitoring of wound healing. Burn wound healing was evaluated by measuring wound area diameter and observing granulation tissue formation and epithelialization to monitor healing progression. No animals died during the study, and all remained in good health throughout the experiment.

### *Tissue handling and outcomes measures*

After seven days of treatment, the animals were euthanized to evaluate TNF-α and VEGF expression. Anesthesia was induced via an intraperitoneal injection of 0.1 mL ketamine. Euthanasia was conducted by exposing the rats to a 30–70% carbon dioxide atmosphere for 3–7

minutes, gradually increasing the concentration until breathing ceased, followed by an additional minute.

Wound tissue samples were aseptically collected and fixed in 10% neutral buffered formalin at room temperature for 24 hours. Histological processing and embedding were performed following an established protocol [26]. Immunohistochemistry was conducted to evaluate TNF-α and VEGF expression using anti-TNF-α (bs-2081R, Bioss, Woburn, MA, USA) and VEGF-A polyclonal antibody (bs-4572R, Bioss, Woburn, MA, USA) following an established protocol [27]. Tissue sections were analyzed under a Zeiss light microscope (Carl Zeiss, Jena, Germany) at 400× magnification, with each observation recorded separately for statistical evaluation. A sample was considered positive if diffuse expression was detected, and staining intensity was used for grading. TNF-α and VEGF expression levels were assessed using an identical semi-quantitative scoring system. Following established methods, TNF-α expression was identified by brown staining in the cytoplasm of skin cells and classified according to the proportion of stained cells: 0–10% (score 0), 11–25% (score 1), 26–50% (score 2), and 51–100% (score 3) [28]. Similarly, VEGF expression was scored based on the percentage of stained cells: 0–10% (score 0), 10–25% (score 1), 25–75% (score 2), and more than 75% (score 3) [29].

### *Statistical analysis*

A one-way ANOVA, followed by Tukey's post-hoc test, was conducted to compare differences in burn wound diameter reduction among treatment groups. Additionally, the expression of TNF-α and VEGF was analyzed using the Kruskal-Wallis H test to assess statistically significant differences between the groups.

## Antimicrobial activity of methanolic propolis extract against methicillin-resistant *Staphylococcus aureus* (MRSA) and *Pseudomonas aeruginosa*

The antimicrobial activity of a methanolic propolis extract was evaluated against two clinically relevant pathogens: methicillin-resistant *Staphylococcus aureus* (MRSA) and *P. aeruginosa*. These organisms were selected due to their significance in healthcare-associated infections and their known resistance to multiple antibiotics. The study utilized Mueller-Hinton agar (MHA) plates, a standard medium for antibiotic susceptibility testing, to ensure reliable and reproducible results.

In the initial phase, MHA plates were evenly inoculated with bacterial suspensions (~$1.5\times10^8$ colony-forming units (CFU)/mL) to ensure uniform growth. A 50 µL (715 µg/µL) volume of 100% propolis extract was added to 6 mm wells. After 18–24 hours of incubation at 37°C, inhibition zones were measured to evaluate the extract's antibacterial activity. After incubating the plates at 37°C for 18–24 hours, the inhibition zones (areas where bacterial growth was prevented) were measured to assess the extract's efficacy. The inhibition zone diameters from the initial assay were used to evaluate the antibacterial activity of the propolis extract. Zones exceeding 12 mm were classified as very strong, those between 8 and 12 mm as strong, zones ranging from 4 to 8 mm as moderate, and those less than 4 mm as weak, following the established criteria [30].

### *Minimum inhibitory concentration determination*

To quantify antimicrobial potency, the propolis extract was serially diluted from 10% to 100% in 10% increments. Each dilution was mixed with a bacterial suspension standardized to 0.5 McFarland turbidity (~$1.5\times10^8$ CFU/mL), ensuring a consistent bacterial load. The mixtures were incubated for 24 hours to determine the minimum inhibitory concentration (MIC). After incubation, aliquots from each dilution were streaked onto fresh MHA plates and incubated again at 37°C for 24 hours. The MIC was recorded as the lowest dilution at which no bacterial colonies were detected.

### *Statistical analysis*

The statistical analysis employed a polynomial regression approach to establish the mathematical relationship between propolis concentration and inhibition zone diameter. Raw data were initially assessed for normality using the Shapiro-Wilk test. A third-degree polynomial regression model was selected after comparing the Akaike Information Criterion (AIC) and Bayesian Information Criterion (BIC) values across polynomial models of different degrees (1–4). The

chosen model was expressed as: Inhibition Zone=$\beta_0+\beta_1$(Concentration)+$\beta_2$(Concentration$^2$)+$\beta_3$(Concentration$^3$). Model parameters were estimated using the ordinary least squares (OLS) method, implemented through the statsmodels Python library.

The goodness of fit was evaluated using multiple statistical metrics: coefficient of determination ($R^2$), adjusted $R^2$ (accounting for the number of predictors), root mean square error (RMSE), and residual analysis. Residuals were examined for homoscedasticity using the Breusch-Pagan test and for autocorrelation using the Durbin-Watson test. The MIC values were determined by numerically solving the regression equation for the concentration at which the predicted inhibition zone equals 1 mm. Confidence intervals (95%) for the MIC estimates were calculated using bootstrapping with 1000 resamples. The statistical significance of the regression coefficients was assessed using t-tests. Cross-validation using a leave-one-out approach was performed to validate the model's predictive accuracy.

The Pearson correlation was applied to assess the relationship between antimicrobial agent concentration (propolis extract and meropenem) and inhibition zone diameter. Initially, data linearity and normality were verified using scatter plots and a normality test (such as the Shapiro-Wilk test). The Pearson correlation coefficient was then calculated for each set of paired values (concentration and inhibition zone diameter) to determine the strength of their relationship. Finally, a two-tailed test was conducted to evaluate the statistical significance of the observed correlation, ensuring it was unlikely to have occurred by chance.

## Propolis metabolite profiling

In this study, liquid chromatography-tandem mass spectrometry (LC-MS/MS) analysis was performed using a Waters 2D UPLC System coupled with a Q Exactive HF High-Resolution Mass Spectrometer (Thermo Fisher Scientific, USA) for metabolite separation and detection. Chromatographic separation was achieved on a Waters ACQUITY UPLC BEH C18 column (1.7 µm, 2.1 mm × 100 mm) at 45°C, with a mobile phase consisting of 0.1% formic acid and acetonitrile in positive ion mode, and ammonium formate with acetonitrile in negative mode. Mass spectrometry settings included a spray voltage of 3.8/−3.2 kV, a full scan range of 70–1050 m/z, and a resolution of 70,000. The top three precursors were selected for MS/MS fragmentation with collision energies of 20, 40, and 60 eV. The system was controlled by Xcalibur software [31].

The raw data collected by LC-MS/MS were processed using Compound Discoverer 3.3 (Thermo Fisher Scientific, Waltham, MA, USA). The data processing steps included peak extraction, retention time correction within and between groups, adduct ion combination, missing value imputation, background peak labeling, and metabolite identification. The resulting data provided molecular weight, retention time, peak area, and identification results. Metabolites were identified using both the BGI Library (Beijing Genomics Institute, Shenzhen, China) and the Thermo mzCloud database (https://www.mzcloud.org) [31].

## Network pharmacology analysis on the anti-inflammatory activity of propolis

Bioactive compounds in propolis were identified using LC-MS/MS, and their simplified molecular-input line-entry system (SMILES) sequences were retrieved from PubChem (https://pubchem.ncbi.nlm.nih.gov). These sequences are critical for subsequent in-silico analysis, as they enable the prediction of compound roles and the identification of protein targets based on structural similarity.

ADMETLab [32] was utilized to forecast the compounds' absorption, distribution, metabolism, excretion, and toxicity (ADMET) characteristics. Meanwhile, Lipinski's Rule of Five (Ro5) [33] was applied to evaluate the drug-likeness of these compounds by examining key factors, such as molecular weight and hydrogen bonding properties.

Target prediction for the bioactive compounds was performed using the SEA Search Server (https://sea.bkslab.org/) [34]. The predicted targets were then filtered based on *p*-value and structural similarity [35,36] to retain only the most relevant associations. These refined targets were further linked to wound healing-related proteins using information from GeneCards (https://www.genecards.org/) and Open Targets (https://www.opentargets.org/). The intersections of these datasets were subsequently visualized using a Venn diagram [37] to identify common targets.

Protein-protein interaction (PPI) analysis was performed on the overlapping targets using STRING (https://string-db.org/). The resulting interaction network was visualized using Cytoscape [38], allowing for a comprehensive examination of the relationship between proteins. Centrality analysis was conducted using CytoHubba, a Cytoscape plugin, to pinpoint hub proteins within the network. Key centrality metrics, such as stress, degree centrality, betweenness centrality, and closeness centrality, were calculated to determine the proteins that play crucial roles in the underlying biological processes [35].

Finally, functional annotation of the genes identified from the Venn diagram was carried out using the Database for Annotation, Visualization, and Integrated Discovery (DAVID) [39]. Only genes with a false discovery rate (FDR) below 0.05 were considered, and their biological roles were further explored using Gene Ontology (GO) terms (https://davidbioinformatics.nih.gov). GO terms provide a standardized vocabulary for describing gene functions across organisms and are divided into three main categories: biological processes (the series of events or molecular functions in which a gene product is involved), cellular components (the specific locations within the cell where a gene product functions), and molecular functions (the biochemical activities of the gene product). This comprehensive network pharmacology approach provided a detailed understanding of the anti-inflammatory activity of propolis, from compound identification to target validation and functional annotation.

# Results

## Wound area and microscopic characteristics of burn wounds

Measurements of burn wound areas on Day 7 revealed significant differences between the treatment groups (**Figure 1**). The propolis-treated group had the smallest average wound diameter at 0.87 cm, indicating a potentially more effective healing process.

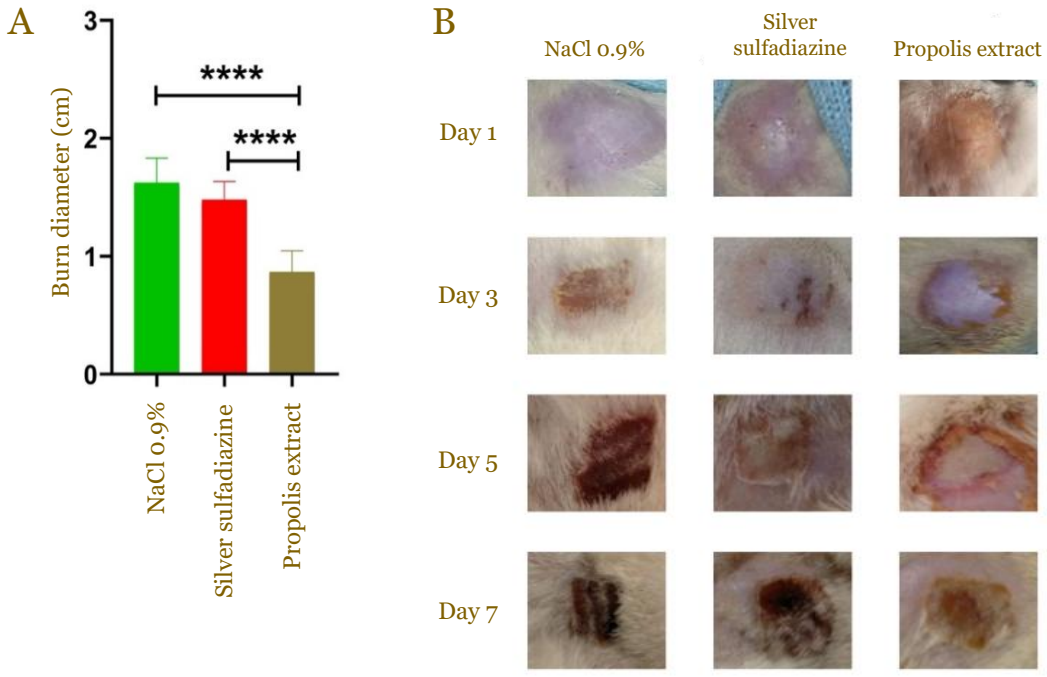


Figure 1. Effect of stingless bee propolis on wound healing. (A) Burn wound diameter after the 7th day of treatment (n=9), statistical analysis by one-way ANOVA followed by Tukey's post-hoc test; **** statistically significant at $p<0.0001$. (B) Representative macroscopic observations of rat skin after deep superficial burns on days 1, 3, 5, and 7, treated with NaCl, silver sulfadiazine, and propolis.

In contrast, the wounds treated with 1% silver sulfadiazine and 0.9% NaCl had larger average diameters of 1.49 cm and 1.61 cm, respectively, suggesting a slower or less efficient healing process with these treatments (**Figure 1A**). These results indicate that propolis extract may lead to more favorable outcomes in reducing burn wound size compared to the other treatments.

The burn wounds treated with the methanolic extract of propolis appeared white-red, with the formation of a thin scab. In comparison, wounds treated with 1% silver sulfadiazine and 0.9% NaCl appeared darker, with a thicker scab. After seven days of treatment, tissue excision was performed on the rats and granulation tissue was evident in all wounds treated with propolis, silver sulfadiazine, and 0.9% NaCl (**Figure 1B**). On a macroscopic level, the burn wounds treated with propolis had a reddish appearance, whereas wounds treated with 1% silver sulfadiazine and 0.9% NaCl were darker and showed scab development.

## Anti-inflammatory activity of propolis

### *TNF-α expression in burn wound healing*

Our data indicated a clear hierarchy in TNF-α expression intensity among the three treatments (**Figure 2A**). The lowest median intensity with minimal variability was observed in the propolis group, while silver sulfadiazine exhibited a moderate intensity with a notable spread. The highest median intensity, along with the largest range, was recorded in the 0.9% NaCl group. Similarly, the scatter plot revealed distinct distribution patterns (**Figure 2B**). Propolis was clustered in the lower scoring and intensity ranges, silver sulfadiazine was more widely dispersed, and 0.9% NaCl was concentrated in the higher intensity range, with scores between 2.0 and 4.0.

Immunohistochemical grading further delineated these patterns. The highest TNF-α expression was observed at lower grading scores (0–25% of cells) in the propolis group, with a decrease at higher scores, suggesting effective regulation of the inflammatory response during healing. In contrast, silver sulfadiazine peaked at moderate grading (26–50% of cells), indicating a more sustained inflammatory phase, while the highest expression was detected in the 0.9% NaCl group at the highest grading score (51–100% of cells), reflecting a prolonged inflammatory phase and potentially delayed healing.

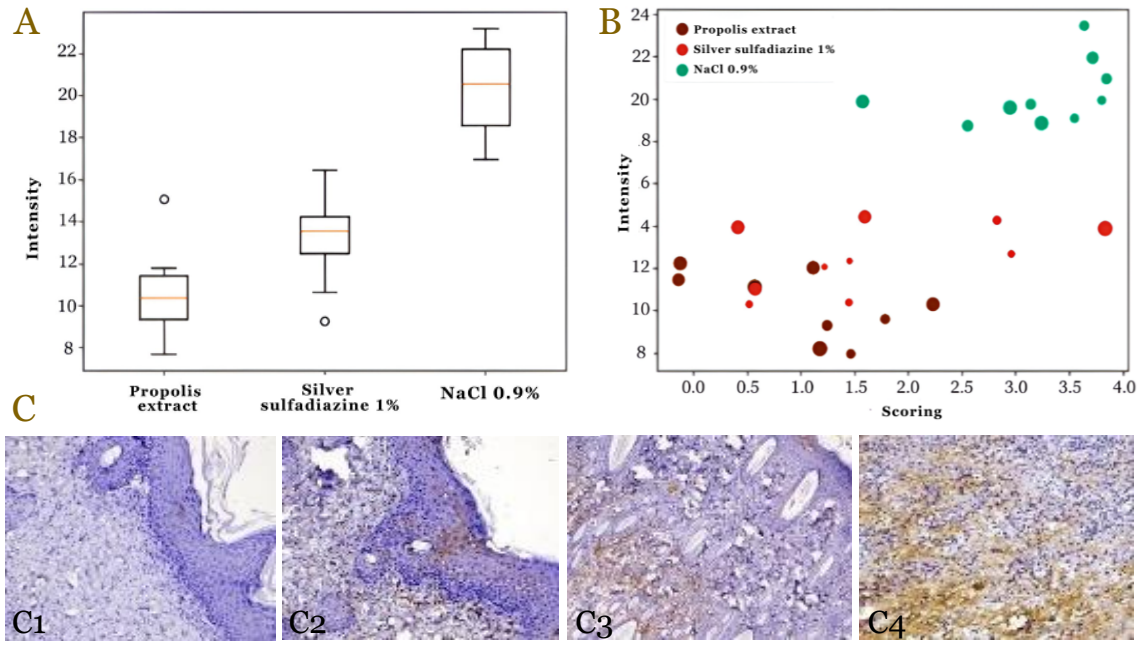


Figure 2. Effect of stingless bee propolis on TNF-α expression in burn wound healing. (A) Box plot comparing TNF-α expression intensity among groups treated with propolis, silver sulfadiazine, and 0.9% NaCl. (B) Scatter plot showing the relationship between scoring and TNF-α expression intensity measurements for propolis (brown), silver sulfadiazine (red), and 0.9% NaCl (green). (C) Representative TNF-α expression in burn wounds on Day 7 according to grading scores, with brown indicating positive staining: (C1) score 0: 0–10% of cells stained, (C2) score 1: 11–25% of cells stained, (C3) score 2: 26–50% of cells stained, and (C4) score 3: 51–100% of cells stained.

Statistical analysis using the Kruskal-Wallis H test confirmed significant differences between the groups ($p$=0.013), with mean ranks of 9.67 for propolis, 12.44 for silver sulfadiazine, and 19.89 for 0.9% NaCl. Post-hoc testing further validated that TNF-α expression was significantly

reduced by propolis ($p$=0.004) compared to silver sulfadiazine ($p$=0.038), while no significant difference was observed between silver sulfadiazine and 0.9% NaCl ($p$=0.438). Collectively, these findings suggest that propolis most effectively modulated the inflammatory response in burn healing by limiting TNF-α expression, potentially offering superior therapeutic benefits compared to conventional treatments.

## VEGF expression and inflammatory response in burn wound healing

Significant differences in VEGF expression among the three treatments were observed (**Figure 3**). The highest median VEGF intensity (~20) was exhibited by propolis, with a narrow interquartile range (18–21) and minimal variability, while the lowest median intensity (~11) was observed with silver sulfadiazine, which also showed a narrow distribution (**Figure 3A**). An intermediate median intensity (~14) with the widest variability was displayed by 0.9% NaCl. Complementary evidence is provided by the scatter plot (**Figure 3B**), in which high VEGF intensities (18–22) were predominantly achieved at lower scoring levels (0–1) by propolis (blue), suggesting robust early-stage expression. In contrast, moderate VEGF expression at mid-range scores (1–2) was primarily associated with silver sulfadiazine (red), and 0.9% NaCl (green) was found to cluster at higher scoring levels (3–4) with moderate intensity, reflecting a delayed or prolonged response.

These differences were confirmed by statistical analysis using the Kruskal-Wallis H test ($p$=0.027), with mean ranks of 19.50 for propolis, 11.78 for NaCl, and 10.72 for silver sulfadiazine. Furthermore, the differences were validated by post hoc tests, which indicated that there was a significant difference between propolis and NaCl 0.9% ($p$=0.0002) as well as between propolis and silver sulfadiazine ($p$=0.0008), while no significant difference was observed between NaCl 0.9% and silver sulfadiazine. These findings support the idea that propolis yields the highest VEGF expression, with silver sulfadiazine producing the lowest, and NaCl 0.9% falling in between.

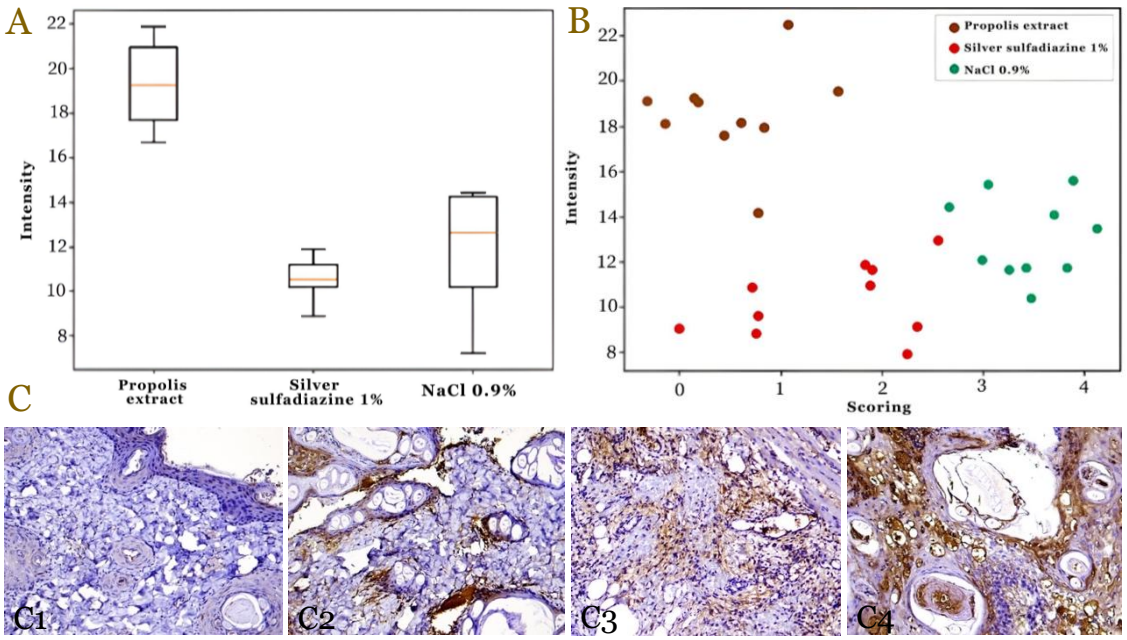


Figure 3. Effect of stingless bee propolis on vascular endothelial cell growth factor (VEGF) expression. (A) The box plot shows that propolis exhibited the highest median VEGF intensity (~20) with minimal variability, while silver sulfadiazine had the lowest (~11). 0.9% NaCl had an intermediate intensity (~14) with the widest variability. (B) The scatter plot indicates that high VEGF expression (18–22) occurred at lower scores (0–1) for propolis (brown), suggesting early-stage upregulation. Silver sulfadiazine (red) showed moderate expression at mid-range scores (1–2), while 0.9% NaCl (green) clustered at higher scores (3–4), indicating a delayed response. (C) The representative VEGF expression in burn wounds on day 7 according to grading scores, with brown indicating positive staining: (C1) score 0: 0–10% of cells stained; (C2) score 1: >10–25% of cells stained; (C3) score 2: >25–75% of cells stained; and (C4) Score 3: >75% of cells stained.

## Antibacterial activity of propolis extract against MRSA and *P. aeruginosa*

The antibacterial activity of methanolic propolis extract was tested against MRSA and *P. aeruginosa* at various concentrations, and the results are presented in **Table 1**. For MRSA, strong inhibition was observed at 100% concentration (715 µg/µL) with a 9 mm inhibition zone, decreasing to moderate inhibition at 90% (7 mm) and 80% (4 mm). The effect diminished significantly below 70%, with inhibition at 70% (4 mm) and weak inhibition at 30% (1 mm), while concentrations below 20% showed no antibacterial activity. Similarly, for *P. aeruginosa*, strong inhibition was observed at 100% (8 mm), with moderate inhibition at 90% (7 mm) and 80% (6 mm). The effect remained moderate at 70% (5 mm) and 60% (4 mm), but weakened below 50%, with only 1 mm inhibition at 30%, and no effect below 20%.

Statistical analysis confirmed that propolis concentration significantly influenced inhibition zone diameters for both MRSA and *P. aeruginosa* (ANOVA, $p$=0.0003), and no significant difference was found between the two bacteria ($t$-test, $p$=0.288). On average, *P. aeruginosa* exhibited slightly larger inhibition zones (5.00 mm) than MRSA (3.56 mm), with greater variability observed in the latter.

Table 1. Inhibition zone diameters and growth inhibition response of methicillin-resistant *Staphylococcus aureus* (MRSA) and *Pseudomonas aeruginosa* at different concentrations of methanolic propolis extract

| Indicator bacteria | Concentration of propolis extract (%)[a] | Average inhibition zone diameter (mm) | Growth inhibition response[b] |
|---|---|---|---|
| MRSA | 100 | 9±0.15 | Strong |
| | 90 | 7±0.25 | Moderate |
| | 80 | 4±0.18 | Moderate |
| Meropenem 10 µg | | 19±0.05 | Very strong |
| *P. aeruginosa* | 100 | 8±0.09 | Strong |
| | 90 | 7±0.05 | Moderate |
| | 80 | 6±0.10 | Moderate |
| Meropenem 10 µg | | 16±0.05 | Very strong |
| MRSA | 70 | 4±0.43 | Moderate |
| | 60 | 3±0.21 | Weak |
| | 50 | 2±0.11 | Weak |
| *P. aeruginosa* | 70 | 5±0.27 | Moderate |
| | 60 | 4±0.19 | Moderate |
| | 50 | 3±0.22 | Weak |
| | 40 | 2±0.08 | Weak |
| MRSA | 40 | 2±0.05 | Weak |
| | 30 | 1±0.10 | Weak |
| | 20 | 0 | No inhibition |
| | 10 | 0 | No inhibition |
| *P. aeruginosa* | 30 | 1±0.20 | Weak |
| | 20 | 0 | No inhibition |
| | 10 | 0 | No inhibition |

[a]100% concentration of propolis corresponds to 715 µg/µL
[b]Antibacterial strength is categorized as strong, moderate, weak, or no inhibition based on the zone size based on previous established criteria [30].

The comparative analysis of propolis extract and meropenem against MRSA and *P. aeruginosa* reveals compelling insights into their antimicrobial efficacy (**Figure 4**). Both agents demonstrated strong positive correlations between concentration and inhibition zone diameter across both bacterial strains, indicating consistent dose-dependent antimicrobial activity. For MRSA, propolis extract had a robust Pearson correlation coefficient of 0.95 ($p$<0.001), while meropenem showed a stronger correlation of 0.979 ($p$<0.001).

Similarly, against *P. aeruginosa*, propolis extract demonstrated a strong correlation of 0.996 ($p$<0.001), with meropenem following closely at 0.984 ($p$<0.001). Notably, both agents demonstrated complete loss of inhibitory activity at the lowest concentration tested (10%), establishing a clear minimum threshold for antimicrobial efficacy. These findings suggest that while propolis extract had genuine antimicrobial properties against both pathogens with highly predictable dose-response relationships, meropenem had superior potency, achieving

approximately 2.5–3 times larger inhibition zones at comparable concentrations, consistent with its established role as a powerful broad-spectrum antibiotic in clinical practice.

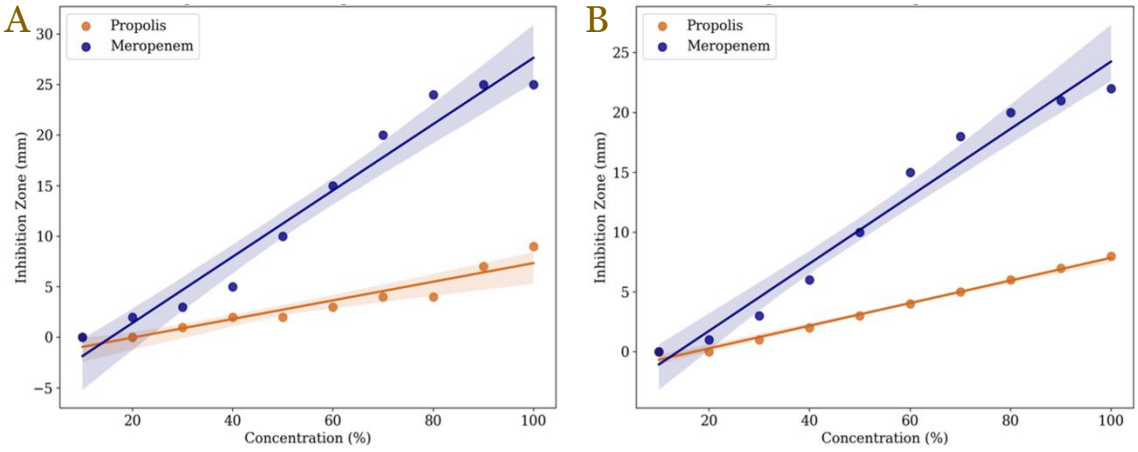


Figure 4. Scatter plots displaying inhibition zones (mm) as a function of concentration (%) with fitted regression lines and confidence intervals. (A) Against methicillin-resistant *Staphylococcus aureus* (MRSA), meropenem demonstrated a stronger correlation ($r$=0.979) than propolis extract ($r$=0.95), with consistently larger inhibition zones at equivalent concentrations. (B) For *P. aeruginosa*, propolis extract exhibited a perfect correlation ($r$=0.996) between concentration and inhibition zone, while meropenem showed a slightly lower correlation ($r$=0.984). At comparable concentrations to those of propolis, meropenem yielded larger inhibition zones, reflecting its greater potency.

### *Minimum inhibitory concentration (MIC) of propolis extract against MRSA and P. aeruginosa*

The MIC values determined through polynomial regression were 27.7% (95%CI: 25.9–29.5%) equivalent to 198.66 µg/µL against MRSA and 29.7% (95%CI: 28.6–30.8%) equal to 212.06 µg/µL against *P. aeruginosa*, slightly lower than the experimentally observed MIC (30% for both strains) (**Figure 5**). Cross-validation confirmed model robustness, with mean absolute percentage errors of 4.2% for MRSA and 2.8% for *P. aeruginosa*.

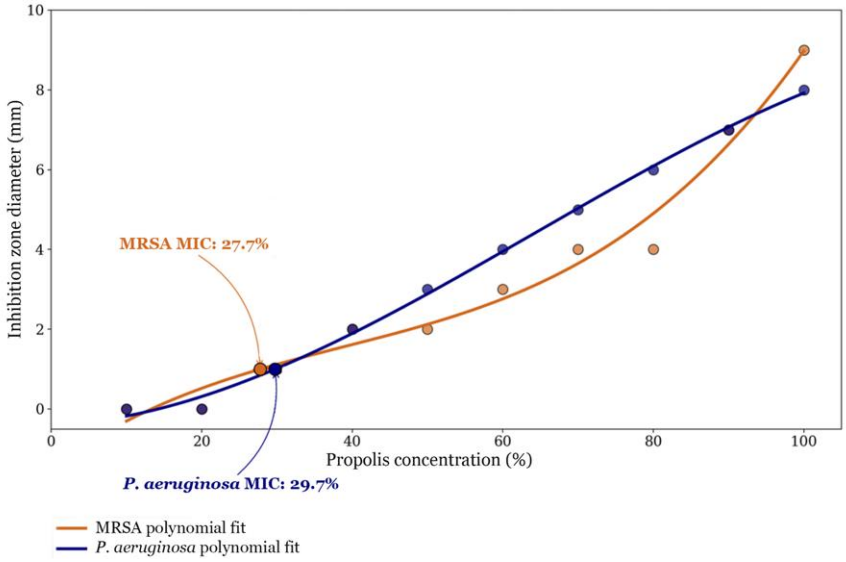


Figure 5. Minimum inhibitory concentration (MIC) of propolis extract against methicillin-resistant *Staphylococcus aureus* (MRSA) and *Pseudomonas aeruginosa*. Polynomial regression estimated the MIC values of 27.7% (equivalent to 198.66 µg/µL) for MRSA and 29.7% (equal to 212.06 µg/µL) for *P. aeruginosa*, slightly lower than the observed 30%. Cross-validation confirmed model robustness, with a low error rate. Residual analysis showed no significant heteroscedasticity or autocorrelation, validating model assumptions. High $R^2$ values (>97%) indicate strong reliability for MIC determination.

Residual analysis indicated no significant heteroscedasticity (Breusch-Pagan test, $p>0.05$) or autocorrelation (Durbin-Watson test, values near 2), validating model assumptions. The high $R^2$ values confirmed that the polynomial models explained over 97% of the variance in inhibition zone measurements, supporting their reliability for MIC determination.

## Metabolite profile of propolis

The metabolite profile of propolis obtained from LC-MS/MS analysis revealed a total of 2,368 detected metabolites, which, after filtering for duplicates and contaminants, resulted in 1,647 unique compounds. These metabolites include a wide range of compound types, such as vitamins (4-pyridoxic acid, a vitamin B6 metabolite), hormones (aldosterone), sugars and carbohydrates (lactose, ribose), organic acids (isocitric acid, oxoglutaric acid), and nucleotide sugars (UDP-N-acetylglucosamine). The findings suggested the presence of phenolic compounds, flavonoids, organic acids, vitamins, hormones, and nucleotide derivatives, highlighting the chemical diversity of propolis.

## Results of network pharmacology analysis on the anti-inflammatory activity of propolis

The ADME assessment revealed that 1,199 of the 1,647 propolis compounds analyzed showed favorable oral bioavailability, as they adhered to Lipinski's rule of five, indicating no violations. Through protein target prediction analysis, 857 target proteins of propolis were identified ($p<0.05$, Tanimoto coefficient >0.5), along with 2,310 wound healing-associated genes. The overlap between these two datasets resulted in 428 targets linked to both bioactive propolis and wound healing processes (**Figure 6**).

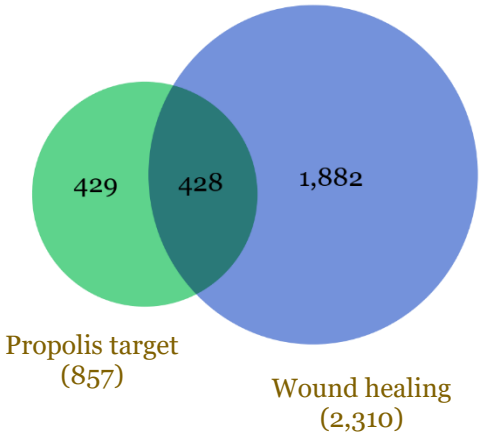


Figure 6. Prediction of protein targets of compounds in propolis related to wound healing. A total of 428 targets linked to both bioactive propolis and wound healing processes.

The results of a STRING-Cytoscape protein-protein interaction analysis for bioactive propolis target proteins related to wound healing are presented in **Figure 7**. Protein nodes are colored by degree centrality, with darker nodes indicating higher centrality, which reflects the number of interactions a protein has within the network. Proteins with high centrality are crucial in the pathway and targeting them with bioactive propolis may modulate key interactions involved in wound healing. Proto-oncogene tyrosine-protein kinase Src (SRC) and E1A binding protein P300 (EP300) exhibited the highest degree centrality, positioning them as crucial regulators in signal transduction and histone modification. Other notable proteins, such as Signal transducer and activator of transcription 3 (STAT3), estrogen receptor 1 (ESR1), heat shock protein 90 alpha family class A member 1 (HSP90AA1), histone deacetylase (HDAC1), protein kinase A catalytic subunit alpha cAMP-activated (PRKACA), JUN proto-oncogene, AP-1 transcription factor subunit (JUN), nuclear factor kappa B subunit 1 (NFKB1), RELA proto-oncogene NF-KB subunit (RELA), tumor necrosis factor (TNF), and mitogen-activated protein kinase 8 (MAPK8), are involved in immune response, inflammation, gene regulation, and cell cycle control. These findings suggested that bioactive propolis compounds may modulate critical

pathways, particularly those involved in inflammation and cellular regulation, underscoring their therapeutic potential.

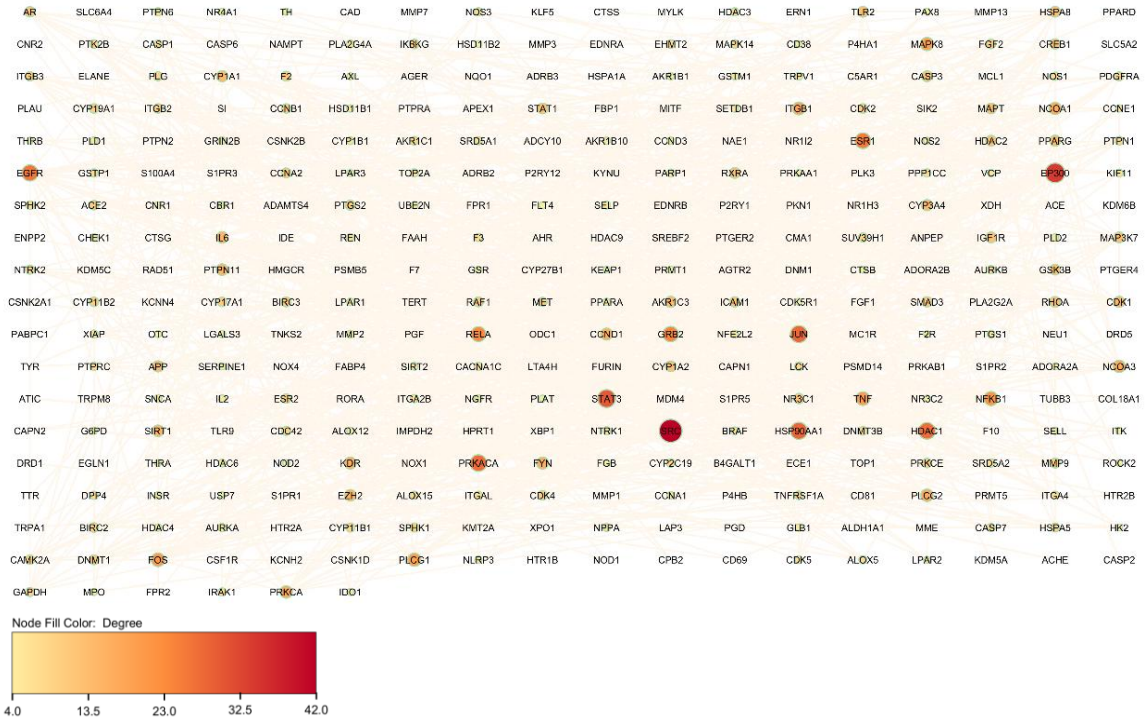


Figure 7. Protein-protein interaction network of bioactive propolis protein targets related to wound healing. Node color indicates connectivity, with yellow for low-degree nodes and red for highly connected, influential nodes. Node size corresponds to connectivity, where larger nodes represent key drug targets.

Alongside degree centrality calculations, shortest path analysis was performed using closeness centrality (CC), which measures how efficiently information can flow from one node to others (ranging from 0 to 1, with higher values being more favorable). Nodes with higher CC values are more easily reachable within the network. Degree centrality (DC) and CC were used to assess a node's significance based on its interactions within the network. Consequently, 20 proteins (SRC, EP300, STAT3, HSP90AA1, JUN, PRKACA, HDAC1, epidermal growth factor receptor (EGFR), ESR1, TNF, integrin subunit beta 1 (ITGB1), protein kinase C alpha (PRKCA), amyloid beta precursor protein (APP), cytochrome P450 1a2 (CYP1A2), prostaglandin-endoperoxide synthase 2 (PTGS2), coagulation factor II (F2), angiotensin-converting enzyme 2 (ACE2), glyceraldehyde-3-phosphate dehydrogenase (GAPDH), plasminogen (PLG), and fibrinogen beta chain (FGB)) were found to have a degree >3, closeness centrality >0.2, and betweenness centrality >0.037 (**Figure 8**).

The network analysis revealed two distinct clusters among the top 20 hub proteins involved in wound healing (**Figure 8**). One cluster comprised transcription factors and signaling regulators (STAT3, JUN, RELA) that coordinate inflammatory and proliferative responses, while the other centered on metabolic and steroid-related enzymes (CYP family members) governing hormonal and metabolic pathways. The red-to-yellow color gradient indicates protein connectedness, with red nodes having more connections. The minimal cross-linking between the clusters highlights their separate yet complementary roles in the wound-healing process (**Figure 8**).

Functional analysis indicated that propolis exhibited the highest potential in modulating the inflammatory response (**Figure 9**), as evidenced by the smallest *p*-value. Additionally, investigation into biological processes revealed that propolis significantly contributed to wound healing mechanisms, including platelet activation, angiogenesis, and apoptosis. Data suggest that propolis might act by binding to proteins predominantly located in the cytoplasm, which play crucial roles in wound healing processes, especially in mediating inflammation.

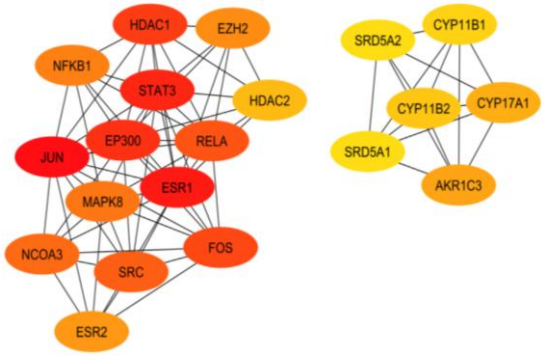


Figure 8. The top 20 hub proteins identified through CytoHubba analysis of the protein-protein interaction network targeting bioactive propolis proteins associated with wound healing. Node color represents connectivity, with yellow indicating low-degree nodes (fewer connections) and red denoting highly connected, influential nodes. More connected nodes (red) are likely key regulators or drug targets in the network. AKR1C3: aldo-keto reductase family 1 member C3, CYP11B1: cytochrome P450 family 11 subfamily B member 1, CYP11B2: cytochrome P450 family 11 subfamily B member 2, CYP17A1: cytochrome P450 family 17 subfamily A member 1, EP300: E1A binding protein P300, ESR1: estrogen receptor 1, ESR2: estrogen receptor 2, EZH2: enhancer of zeste homolog 2, FOS: proto-oncogene c-Fos, HDAC1: histone deacetylase 1, HDAC2: histone deacetylase 2, JUN: jun proto-oncogene, MAPK8: mitogen-activated protein kinase 8; NCOA3: nuclear receptor coactivator 3; NFKB1: nuclear factor kappa B subunit 1, RELA: RELA proto-oncogene NF-KB subunit, SRC: proto-oncogene tyrosine-protein kinase Src, SRD5A1: steroid 5 alpha-reductase 1, SRD5A2: steroid 5 alpha-reductase 2, STAT3: signal transducer and activator of transcription 3.

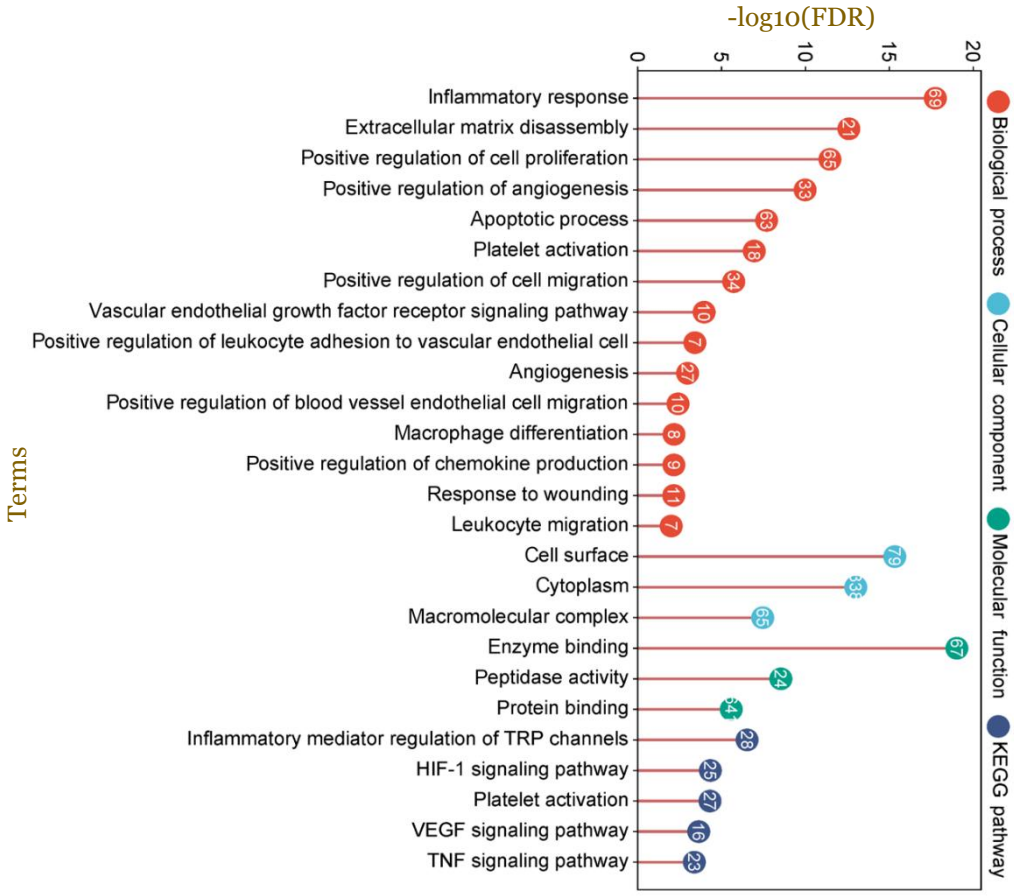


Figure 9. Functional enrichment analysis of bioactive propolis protein targets related to wound healing with a *p*-value of <0.01. The x-axis represents the -$\log_{10}$(false discovery rate (FDR)), indicating the statistical significance of enriched terms. The y-axis lists biological processes, cellular components, molecular functions, and Kyoto Encyclopedia of Genes and Genomes (KEGG) pathways. Red circles denote biological processes, light blue circles represent cellular components, green circles indicate molecular functions, and dark blue circles correspond to KEGG pathways.

The enrichment analysis reveals significant involvement of immune responses, cell proliferation, and key signaling pathways. The most enriched process is the inflammatory response, followed by extracellular matrix disassembly, cell proliferation, and angiogenesis, all crucial for tissue remodeling and tumor growth. Immune system activation is also highlighted by terms related to leukocyte migration and adhesion. On a cellular level, active intracellular transport and complex formation are indicated, while molecular functions point to immune signaling and enzyme interactions. Key pathways include the TNF, VEGF, and HIF-1 signaling pathways, which regulate inflammation, blood vessel formation, and responses to hypoxia. These findings suggest a focus on immune responses, inflammation, and tissue growth, commonly linked to chronic inflammation, regeneration, and cancer.

## Discussion

The results of this study provide convincing evidence for the synergistic anti-inflammatory and antimicrobial effects of stingless bee propolis in treating second-degree burns, as suggested by its dual capacity to modulate inflammatory responses and exhibit antimicrobial action. This synergy is critical for optimizing wound healing, where the control of inflammation and the prevention of infection are both necessary for successful recovery. Propolis appears not only to reduce inflammation but also to effectively prevent bacterial colonization, which is a significant factor in burn wound care. This combined action of propolis suggests that it offers a more comprehensive therapeutic approach than conventional treatments like silver sulfadiazine and 0.9% NaCl, which generally address either inflammation or infection, but not both simultaneously.

The modulation of TNF-α levels in the propolis-treated group suggests that propolis may offer superior anti-inflammatory effects, leading to improved healing outcomes. In contrast, the higher TNF-α expression in the NaCl-treated group reflects a prolonged inflammatory response and slower recovery. TNF-α plays a dual role as a pro-inflammatory cytokine and in tissue repair by regulating the expression of VEGF, which is essential for angiogenesis [40]. VEGF promotes the formation of new blood vessels, supplying oxygen and nutrients to the injury site, and TNF-α further enhances tissue repair by increasing mesenchymal stem cells (MSCs) migration and adhesion. This combination of MSC mobilization and VEGF-driven angiogenesis highlights TNF-α's central role in wound healing [40-43].

Propolis has been reported to exhibit tumor-preventive and anti-inflammatory effects by inhibiting NF-κB and associated signaling pathways, including toll-like receptor 4 (TLR4), myeloid differentiation primary response 88 (MyD88), interleukin-1 receptor-associated kinase 4 (IRAK4), TIR-domain-containing adapter-inducing interferon-β (TRIF), and NOD-like receptor family, pyrin domain-containing 3 (NLRP3) inflammasomes [44]. This inhibition leads to the downregulation of pro-inflammatory cytokines, including interleukin-1 (IL-1), interleukin-6 (IL-6), interferon-gamma (IFN-γ), and TNF-α [19,44]. In the context of this study, propolis's ability to modulate TNF-α and enhance VEGF expression suggests it can simultaneously control inflammation and support angiogenesis, promoting effective wound healing. This highlights TNF-α's dual role in driving inflammation and regulating tissue repair, emphasizing the need for balance between inflammation and regeneration necessary for optimal healing.

Network pharmacology analysis further supports these findings by identifying key proteins such as JUN, ESR1, STAT3, and SRC, which are linked to the regulation of TNF-α and VEGF pathways. JUN, a member of the activated protein-1 (AP-1) family of transcription factors, regulates cellular responses to inflammatory cytokines like TNF-α, influencing gene expression related to immune function and wound healing [45,46]. ESR1, which encodes for estrogen receptor alpha (ERα), has been implicated in modulating immune responses and inflammation [47,48], contributing to the body's ability to respond to injury. STAT3, a central mediator of cytokine signaling, is activated by TNF-α and plays a crucial role in promoting cell survival, proliferation, and angiogenesis by regulating VEGF expression [49]. The involvement of these proteins in both the inflammatory and regenerative phases of wound healing suggests that the bioactive compounds in propolis are capable of modulating multiple molecular pathways to balance inflammation and tissue repair. This multifaceted approach is important in managing complex biological processes like wound healing, where a single treatment can modulate several pathways simultaneously and can offer significant therapeutic advantages.

In this study, SRC and EP300 were identified as crucial nodes within the interaction network, emphasizing their significant roles in cellular signaling and gene regulation. SRC plays a central role in TNF-α-mediated signal transduction pathways and has been shown to upregulate VEGF, thereby promoting angiogenesis in response to tissue injury. Previous research has demonstrated that both SRC and EP300 are essential components in network pharmacology, particularly in their impact on cellular signaling pathways and gene expression regulation [50].

Previous studies have highlighted SRC's pivotal role in angiogenesis by regulating VEGF expression through the TNF-α signaling pathway, promoting blood vessel formation essential for tissue regeneration. TNF-α further contributes to vascular remodeling by directly influencing endothelial cells and other pro-inflammatory mediators [51-53]. Compounds in propolis, which can suppress excessive TNF-α activity, underscore the therapeutic value of targeting these pathways to regulate inflammation and promote tissue healing.

EP300, a histone acetyltransferase, regulates chromatin structure and gene expression, influencing the transcription of genes involved in inflammation and tissue regeneration [54]. While the direct connection between propolis and EP300-mediated gene regulation is still being researched, propolis is well-documented for its ability to modulate inflammatory pathways. It stimulates the production of anti-inflammatory cytokines and inhibits pro-inflammatory cytokines, likely contributing to wound healing. The antioxidant and polyphenolic compounds in propolis further enhance its potential in treating chronic inflammation and promoting tissue repair [55]. Though the exact epigenetic mechanisms remain unclear, propolis's influence on key molecular pathways involved in inflammation suggests that it may support long-term healing outcomes by regulating gene expression through mechanisms like those involving EP300.

The findings of this study suggest that propolis offers a comprehensive therapeutic approach, modulating both TNF-α and VEGF to optimize the wound healing process. By controlling TNF-α levels, propolis may reduce excessive inflammation while enhancing VEGF-mediated angiogenesis, which is essential for supplying blood, oxygen, and nutrients to the regenerating tissue. This dual action—controlling inflammation and promoting tissue regeneration—positions propolis as a potentially superior treatment for second-degree burns and other inflammatory conditions. The ability to influence both inflammatory and regenerative pathways is critical in wound care, as it ensures that inflammation is managed without impeding the body's natural repair mechanisms.

The antibacterial efficacy of propolis against MRSA and *P. aeruginosa* highlights its potential as a broad-spectrum therapeutic agent. MIC results showed that propolis is slightly more effective against MRSA (27.7% MIC) than *P. aeruginosa* (29.7% MIC), confirming its concentration-dependent antibacterial activity. Higher doses effectively inhibited bacterial growth, particularly in drug-resistant strains. These results are consistent with other studies showing that propolis's antimicrobial activity is due to its rich composition of bioactive compounds, such as flavonoids and phenolic acids, which disrupt microbial cell walls and inhibit bacterial enzyme function [56-58].

The antimicrobial properties of propolis enhance its anti-inflammatory and wound-healing effects, creating a comprehensive approach to wound care. In addition to controlling inflammation and promoting tissue repair, propolis prevents infections that could otherwise delay healing. This dual function, serving both as an anti-inflammatory and antimicrobial agent, makes propolis a promising alternative to conventional wound care treatments, especially in burn injuries where infection can severely impact recovery.

## Conclusion

This study demonstrated that stingless bee propolis had a synergistic effect through anti-inflammatory and antimicrobial mechanisms, making it a promising therapeutic agent for second-degree burns. The modulation of TNF-α and VEGF by propolis suggests that it plays a pivotal role in facilitating tissue repair by controlling inflammation and promoting angiogenesis. Network pharmacology analysis further identified key proteins involved in the regulatory pathways of TNF-α and VEGF, highlighting the potential molecular basis of propolis' dual action. Additionally, the potent antimicrobial properties of propolis against MRSA and *P. aeruginosa* highlight its potential in preventing infections in burn wounds, which, when

combined with its anti-inflammatory effects, offer a comprehensive treatment strategy. The ability of propolis to balance inflammation, promote tissue regeneration, and prevent bacterial colonization suggests that it could offer significant clinical advantages over conventional burn treatments. Future research should focus on elucidating the molecular mechanisms through which propolis influences TNF-α and VEGF, as well as exploring its clinical applications in wound care and infection management. Additionally, studies could investigate the specific bioactive compounds in propolis responsible for these effects and explore their potential in other inflammatory and infectious conditions, further expanding the therapeutic scope of propolis in clinical practice.

### Ethics approval

Ethical clearance has been approved under No. KEPK 01/09/208/2023, issued by the Ethics Committee of the Health Polytechnic of the Ministry of Health Manado on September 11, 2023.

### Acknowledgments

The authors gratefully acknowledge the research support and assistance provided by the Directorate of Research, Technology, and Community Service, Ministry of Education, Culture, Research, and Technology, Republic of Indonesia.

### Competing interests

All the authors declare that there are no conflicts of interest.

### Funding

This project was funded under the Doctoral Dissertation Research Scheme, with primary contract number 084/E5/PG.02.00.PL/2024 and derivative contract number 1902/UN12.13/LT/2024.

### Underlying data

Derived data supporting the findings of this study are available from the corresponding author on request.

### Declaration of artificial intelligence use

Manuscript writing support was provided exclusively by ChatGPT, which assisted with language refinement. Matplotlib was used to generate Python code for creating some of the graphical images. We confirm that all AI-assisted processes were critically reviewed by the authors to ensure the integrity and reliability of the results. The final decisions and interpretations presented in this article were solely made by the authors.

## How to cite

Manginstar CO, Tallei TE, Salaki CL, *et al.* Dual anti-inflammatory and antimicrobial effects of stingless bee propolis on second-degree burns. Narra J 2025; 5 (1): e2359 - http://doi.org/10.52225/narra.v5i1.2359.

## References

1. Rogers AD, Jeschke MG. Managing severe burn injuries: Challenges and solutions in complex and chronic wound care. Chronic Wound Care Manag Res 2016;3:59-71.
2. Ji S, Xiao S, Xia Z, *et al.* Consensus on the treatment of second-degree burn wounds (2024 edition). Burns Trauma 2024;12:tkad061.
3. Jeschke MG, van Baar ME, Choudhry MA, *et al.* Burn injury. Nat Rev Dis Primer 2020;6(1):11.
4. Mulder PPG, Vlig M, Fasse E, *et al.* Burn-injured skin is marked by a prolonged local acute inflammatory response of innate immune cells and pro-inflammatory cytokines. Front Immunol 2022;13:1034420.
5. DeJesus JE, Wen JJ, Radhakrishnan R. Cytokine pathways in cardiac dysfunction following burn injury and changes in genome expression. J Pers Med 2022;12(11):1876.
6. Strudwick XL, Cowin AJ. The role of the inflammatory response in burn injury. In: Kartal SP, Bayramgürler D, editors. Hot topics in burn injuries. Rijeka: IntechOpen; 2017.

7. Roy S, Mukherjee P, Kundu S, *et al.* Microbial infections in burn patients. Acute Crit Care 2024;39(2):214-225.
8. Yang Y, Huang J, Zeng A, *et al.* The role of the skin microbiome in wound healing. Burns Trauma 2024;12:tkad059.
9. Zhang P, Zou B, Liou YC, *et al.* The pathogenesis and diagnosis of sepsis post burn injury. Burns Trauma 2021;9:tkaa047.
10. Chen YY, Wu PF, Chen CS, *et al.* Trends in microbial profile of burn patients following an event of dust explosion at a tertiary medical center. BMC Infect Dis 2020;20(1):193.
11. Chuttong B, Lim K, Praphawilai P, *et al.* Exploring the functional properties of propolis, geopropolis, and cerumen, with a special emphasis on their antimicrobial effects. Foods 2023;12(21):3909.
12. Hossain R, Quispe C, Khan RA, *et al.* Propolis: An update on its chemistry and pharmacological applications. Chin Med 2022;17(1):100.
13. Manginstar CO, Tallei TE, Niode NJ, *et al.* Therapeutic potential of propolis in alleviating inflammatory response and promoting wound healing in skin burn. Phytother Res 2024;38(2):856-879.
14. Syed SSNA, Mohd Hanapiah NA, Ahmad H, *et al.* Determination of total phenolics, flavonoids, and antioxidant activity and GC-MS analysis of Malaysian stingless bee propolis water extracts. Scientifica 2021;2021:3789351.
15. Lim JR, Chua LS, Dawood DAS. Evaluating biological properties of stingless bee propolis. Foods 2023;12(12):2290.
16. Xu W, Lu H, Yuan Y, *et al.* The antioxidant and anti-inflammatory effects of flavonoids from propolis via Nrf2 and NF-κB pathways. Foods 2022;11(16):2439.
17. Bhargava P, Mahanta D, Kaul A, *et al.* Experimental evidence for therapeutic potentials of propolis. Nutrients 2021;13(8):2528.
18. Bhatti N, Hajam YA, Mushtaq S, *et al.* A review on dynamic pharmacological potency and multifaceted biological activities of propolis. Discov Sustain 2024;5(1):185.
19. Oršolić N, Jazvinšćak Jembrek M. Molecular and cellular mechanisms of propolis and its polyphenolic compounds against cancer. Int J Mol Sci 2022;23(18):10479.
20. Ruttanapattanakul J, Wikan N, Potikanond S, *et al.* Molecular targets of pinocembrin underlying its regenerative activities in human keratinocytes. Pharmaceuticals 2022;15(8):954.
21. Bouchelaghem S. Propolis characterization and antimicrobial activities against Staphylococcus aureus and Candida albicans: A review. Saudi J Biol Sci 2022;29(4):1936-1946.
22. Zulhendri F, Chandrasekaran K, Kowacz M, *et al.* Antiviral, antibacterial, antifungal, and antiparasitic properties of propolis: A review. Foods 2021;10(6):1360.
23. Rukmana A, Supardi LA, Sjatha F, *et al.* Responses of humoral and cellular immune mediators in BALB/c mice to LipX (PE11) as seed tuberculosis vaccine candidates. Genes 2022;13(11):1954.
24. Cai EZ, Ang CH, Raju A, *et al.* Creation of consistent burn wounds: A rat model. Arch Plast Surg 2014;41:317-324.
25. Balqis U, Frengky, Azzahrawani N, *et al.* Efficacy of cucumber (*Cucumis sativus* L.) on healing of IIB degree burn wound (*Vulnus combustion*) in rat (*Rattus norvegicus*). J Med Vet 2016;10(2):90-93.
26. Slaoui M, Fiette L. Histopathology procedures: From tissue sampling to histopathological evaluation. Methods Mol Biol 2011;691:
69-82.
27. Fathimah FSN, Zuhria I, Lutfi D, *et al.* The anti-inflammatory potential of epigallocatechin gallate (EGCG) on tumor necrosis factor alpha and interleukin–10 expression in pseudomonas keratitis model (in vivo study on *Rattus norvegicus* rats model). Bali Med J 2024;13(2):551-557.
28. Jammal MP, DA Silva AA, Filho AM, *et al.* Immunohistochemical staining of tumor necrosis factor-α and interleukin-10 in benign and malignant ovarian neoplasms. Oncol Lett 2015;9(2):979-983.
29. Loureiro LVM, Neder L, Callegaro-Filho D, *et al.* The immunohistochemical landscape of the VEGF family and its receptors in glioblastomas. Surg Exp Pathol 2020;3(1):9.
30. Husain DR, Gunawan S, Sulfahri S. Antimicrobial potential of lactic acid bacteria from domestic chickens (*Gallus domesticus*) from South Celebes, Indonesia, in different growth phases: In vitro experiments supported by computational docking. Iran J Microbiol 2020;12(1):62-69.
31. Tallei TE, Savitri M, Lee D, *et al.* A comparative analysis on impact of drying methods on metabolite composition in broccoli microgreens. LWT 2024;210:116866.
32. Fu L, Shi S, Yi J, *et al.* ADMETlab 3.0: An updated comprehensive online ADMET prediction platform enhanced with broader coverage, improved performance, API functionality and decision support. Nucleic Acids Res 2024;52(W1):W422-W431.

33. Lipinski CA. Rule of five in 2015 and beyond: Target and ligand structural limitations, ligand chemistry structure and drug discovery project decisions. Adv Drug Deliv Rev 2016;101:34-41.
34. Keiser MJ, Roth BL, Armbruster BN, *et al.* Relating protein pharmacology by ligand chemistry. Nat Biotechnol 2007;25(2):197-206.
35. Tallei T, Fatimawali F, Yelnetty A, *et al.* Unveiling the immunomodulatory mechanisms of pineapple metabolites: A multi-modal computational analysis using network pharmacology, molecul ar docking, and molecular dynamics simulation. J Adv Biotechnol Exp Ther 2024;7(1):1-22.
36. Kairupan TS, Kapantow NH, Tallei TE, *et al.* Mechanistic insights into the anticancer, anti-inflammatory, and antioxidant effects of yellowfin tuna collagen peptides using network pharmacology. Narra J 2025;5(1):e1885.
37. Fatimawali, Tallei TE, Kepel BJ, *et al.* Molecular insight into the pharmacological potential of *Clerodendrum minahassae* leaf extract for type-2 diabetes management using the network pharmacology approach. Medicina 2023;59(11):1899.
38. Shannon P, Markiel A, Ozier O, *et al.* Cytoscape: A software environment for integrated models. Genome Res 2003;13(22):426.
39. Sherman BT, Hao M, Qiu J, *et al.* DAVID: A web server for functional enrichment analysis and functional annotation of gene lists (2021 update). Nucleic Acids Res 2022;50(W1):W216-W221.
40. Li W, Liu Q, Shi JX, *et al.* The role of TNF-α in the fate regulation and functional reprogramming of mesenchymal stem cells in an inflammatory microenvironment. Front Immunol 2023;14:1074863.
41. Everts PA, Lana JF, Onishi K, *et al.* Angiogenesis and tissue repair depend on platelet dosing and bioformulation strategies following orthobiological platelet-rich plasma procedures: A narrative review. Biomedicines 2023;11(7).
42. Tyavambiza C, Meyer M, Meyer S. Cellular and molecular events of wound healing and the potential of silver based nanoformulations as wound healing agents. Bioengineering 2022;9(11):712.
43. Zhu M, Chu Y, Shang Q, *et al.* Mesenchymal stromal cells pretreated with pro-inflammatory cytokines promote skin wound healing through VEGFC-mediated angiogenesis. Stem Cells Transl Med 2020;9(10):1218-1232.
44. Zulhendri F, Lesmana R, Tandean S, *et al.* Recent update on the anti-inflammatory activities of propolis. Molecules 2022;27(23):8473.
45. Diaz-Cañestro C, Reiner MF, Bonetti NR, *et al.* AP-1 (activated protein-1) transcription factor JunD regulates ischemia/reperfusion brain damage via IL-1β (interleukin-1β). Stroke 2019;50(2):469-477.
46. Yin Y, Wang S, Sun Y, *et al.* JNK/AP-1 pathway is involved in tumor necrosis factor-α induced expression of vascular endothelial growth factor in MCF7 cells. Biomed Pharmacother 2009;63(6):429-435.
47. Koning T, Calaf GM. Association of inflammation and immune cell infiltration with estrogen receptor alpha in an estrogen and ionizing radiation-induced breast cancer model. Int J Mol Sci 2024;25(16):8604.
48. Shindo S, Chen SH, Gotoh S, *et al.* Estrogen receptor α phosphorylated at Ser216 confers inflammatory function to mouse microglia. Cell Commun Signal 2020;18(1):117.
49. Wei W, Wang J, Huang P, *et al.* Tumor necrosis factor-α induces proliferation and reduces apoptosis of colorectal cancer cells through STAT3 activation. Immunogenetics 2023;75(2):161-169.
50. Xiao W, Xu Y, Baak JP, *et al.* Network module analysis and molecular docking-based study on the mechanism of astragali radix against non-small cell lung cancer. BMC Complement Med Ther 2023;23(1):345.
51. Baluk P, Yao LC, Feng J, *et al.* TNF-α drives remodeling of blood vessels and lymphatics in sustained airway inflammation in mice. J Clin Invest 2009;119(10):2954-2964.
52. Naito H, Iba T, Takakura N. Mechanisms of new blood-vessel formation and proliferative heterogeneity of endothelial cells. Int Immunol 2020;32(5):295-305.
53. Tigges U, Boroujerdi A, Welser-Alves J V, *et al.* TNF-α promotes cerebral pericyte remodeling in vitro, via a switch from α1 to α2 integrins. J Neuroinflammation 2013;10(1):33.
54. Rubio K, Molina-Herrera A, Pérez-González A, *et al.* EP300 as a molecular integrator of fibrotic transcriptional programs. Int J Mol Sci 2023;24(15):12302.
55. Pahlavani N, Malekahmadi M, Firouzi S, *et al.* Molecular and cellular mechanisms of the effects of Propolis in inflammation, oxidative stress and glycemic control in chronic diseases. Nutr Metab 2020;17(1):65.
56. Devequi-Nunes D, Machado BAS, Barreto G de A, *et al.* Chemical characterization and biological activity of six different extracts of propolis through conventional methods and supercritical extraction. PLoS One 2018;13(12):e0207676.
57. Przybyłek I, Karpiński TM. Antibacterial properties of propolis. Molecules 2019;24(11):2047.
58. Siheri W, Alenezi S, Tusiimire J, *et al.* The chemical and biological properties of propolis. In: Alvarez-Suarez JM, editor. Cham: Springer; 2017.